

# NITROGEN ION IMPLANTATION OF CHROMIUM CONTAINING MARTENSITE STEELS: PRELIMINARY SURFACE PROCESSING AND DOSE RATE INFLUENCE

<sup>(1)</sup>A.V. Byeli, <sup>(2)</sup>V.A. Kukareko, <sup>(1)</sup>A.N. Karpovich

<sup>(1)</sup>Physical-Technical Institute of the NAS of Belarus

<sup>(2)</sup>Joint Institute of Mechanical Engineering of the NAS of Belarus  
Minsk, Belarus, e-mail: vmo@tut.by

**Abstract:** X-ray diffraction, optical and electron microscopy were used to analyze microstructural variations in the surface layers of martensite chromium containing steels after low-energy, high-current-density ion implantation. These data show that nitrogen implantation produces solid solutions and precipitates of new phases in surface layers that are several micrometers thick. Phases formed are controlled by the virgin microstructure of blocks, the temperature of implantation and the ion fluence. The influence of processing length and ion beam current density are also considered.

## Introduction

A unique, promising technique of low-energy ion implantation at ion current densities as high as several milliamperes per square centimeter has been successfully developed over the past few years [1-5]

High-current-density treatment induces significant heating of the surface which facilitates effective diffusive redistribution of implanted atoms thereby combining the benefits of traditional thermo-chemical and ion-beam technologies. The increased concentration of radiation-induced defects (e.g. vacancies) during ion implantation in a surface layer with a thickness around 20-30 nm, favors prompt growth and saturation of a deeper surface layer. The interaction of chemically active alloying elements with implanted atoms can also promote the effective redistribution of impurities.

It was demonstrated elsewhere that low-energy elevated-temperature ion implantation of nitrogen improves dramatically tribological properties of ferrous materials and modifies comparatively deep surface layer. Data have been presented that demonstrate solid solutions, precipitates of new phases and sometimes amorphization of surface layers with thicknesses up to several  $\mu\text{m}$  and more are induced by elevated-temperature low-energy ion implantation. The phases formed are controlled by the implantation parameters, which can be maintained easily and precisely to ensure optimum properties of the surface (Fig. 1). Most of the microstructures, produced by ion implantation are metastable and characterized by increased level of stored energy. This excessive energy can be used for transformation of surface microstructure during friction to optimize tribological properties of the surface.

However, the mechanisms that yield these benefits during high-current-density implantation, the influence of ion beam current density (dose rate) and the virgin structural state of the surface layer on the microstructures and mechanical properties of various implanted metals and alloys are still not well understood.

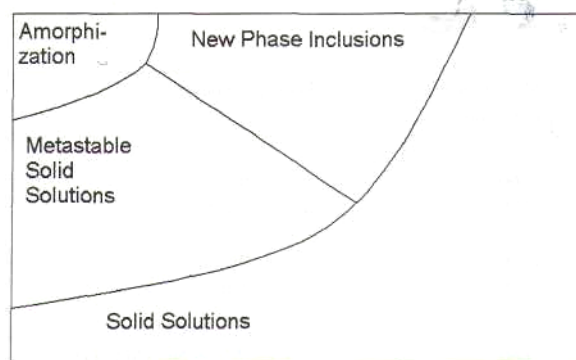


**Fig. 1.** Schematic for phase transformations induced by low-energy elevated-temperature ion implantation.

## Materials and experimental techniques

40X and 40X13 martensite steels were used in the research. Table 1 shows the chemical composition of the surface of steels determined using a scanning electron microscope (Nanolab 7), equipped with an X-ray microanalyzer. The values given are the average of concentrations measured at three different points on a block. Heat treatment prior to implantation involved quenching in oil or annealing (1270 K, 30 min) of blocks. After heat treatment all blocks were ground to  $R_a = 0.4 \mu\text{m}$  so the influence of the surface finish and microstructure on the parameters of the implanted layer could be determined. Nitrogen ions from the gaseous implanter were molecular (approximately 70%) and atomic (approximately 30%). Blocks were implanted with 3 keV nitrogen ions at an ion current density (dose rate) of 1 - 2  $\text{mA}/\text{cm}^2$ . These conditions correspond to integrated fluence of  $1 \times 10^{20}$  ions/ $\text{cm}^2$ . Blocks were held at 670 K during implantation. The temperature was selected on the basis of preliminary research on low-energy, high-current-density ion implantation which demonstrated that 670 K was sufficient to yield a modified surface layer that was several tenths of micrometers thick. The temperatures of the blocks were monitored during implantation using a thermocouple located 2 mm from the surface being treated.

Table 1

Element⇒ Steel↓	C	Cr	Ni	Mn	Fe
40X	0.39	0.95	0.20		Balance
40X13	0,45	13,5	0,5	0,1	Balance

Microhardness was measured at a 25 gf load with a 10 s dwell time. Ten indentations were made on each block so statistically significant mean values could be obtained.

Optical microscopy was used for metallographic study of blocks that were sectioned so the etched edges of the implanted layers could be observed. Samples were etched in an acid mixture of  $\text{HNO}_3$  and  $\text{HCl}$ . X-ray diffraction analysis was carried out to study microstructural changes induced by the ion treatment. Bregg-

Brentano focusing and scanning in  $0.1^\circ$  steps with a fixed counting time (40" per step) were used in the analysis. Standard ASTM data were used for phase identification.

## Results and discussion

Cross-sectional views showing the microstructures near the surface of nitrogen-implanted 40X steel are presented in Fig. 2. The microphotographs show the depth of modified surface

layer exceeded several micrometers for both annealed and quenched steel.

After hardening 40X steel had a martensite structure with the lattice parameter  $a = 0.2872$  nm and surface microhardness  $H_{\mu} = 6700$  MPa. Low-energy nitrogen ion implantation at  $1 \text{ mA/cm}^2$  influences 40-50  $\mu\text{m}$  surface layer (Table 2, Fig. 2,) and increases its microhardness up to  $H = 9900$  MPa. Bulk microhardness of ion implanted steel falls down to  $H = 3700$  MPa. Analysis of X-ray data revealed  $\epsilon\text{-Fe}_2\text{N}$ ,  $\gamma'\text{-Fe}_4\text{N}$  and martensite phases (Fig. 3). Ion implantation at dose rate  $1.5 \text{ mA/cm}^2$  results in significantly thinner nitride surface layer (30 - 40  $\mu\text{m}$ ). The microhardness of the surface falls down to  $H_{\mu} = 9500$  MPa.

After annealing 40X steel had a ferrite-perlite structure consisting of  $\alpha\text{-Fe}$  and  $\text{Fe}_3\text{C}$  with the lattice parameter  $a = 0.2866$  nm and surface microhardness  $H_{\mu} = 2300$  MPa. Nitrogen ion implantation results in continuous 2  $\mu\text{m}$  thick surface layer of

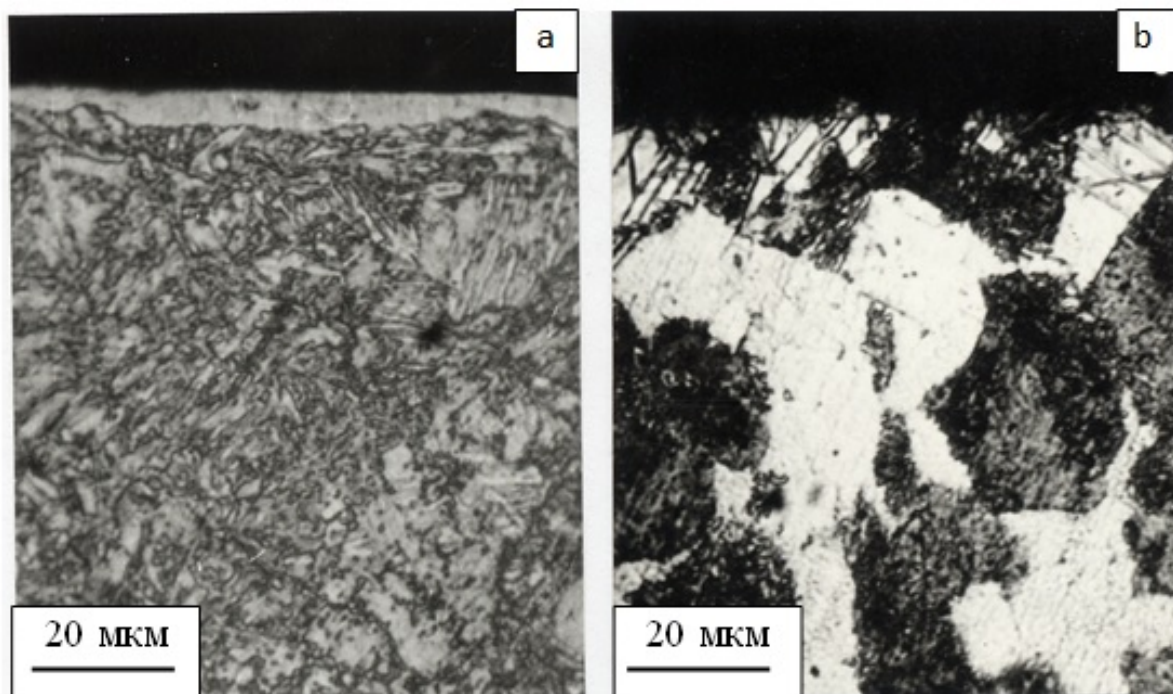
nitrides containing large lamellar nitrides. The doped layer thickness did not exceed 20  $\mu\text{m}$ . X-ray data revealed  $\alpha\text{-Fe}$ ;  $\epsilon\text{-Fe}_{2-3}\text{N}$ ;  $\gamma'\text{-Fe}_4\text{N}$ , and  $\text{Fe}_3\text{C}$  phases. Dose rate did not influence phase composition of doped layer, but dense ion fluxes resulted in low intensities of nitride lines. Surface microhardness fell down up to 6200 and 5800 MPa for dose rates 1.5 and 2  $\text{mA/cm}^2$  correspondingly.

After hardening the unimplanted 40X13 block had a martensite structure with the lattice parameter  $a = 0.2876$  nm and microhardness  $H = 6000$  MPa. Nitrogen ion implantation at  $1 \text{ mA/cm}^2$  influenced 18-20  $\mu\text{m}$  surface layer (Fig. 4) and increased its surface microhardness up to  $H_{\mu} = 12000$  MPa. Bulk microhardness of ion implanted block fell down to  $H_{\mu} = 5000$  MPa. X-ray diffraction of blocks revealed a near-surface layer containing  $\alpha_{\text{N}}$ ,  $\epsilon\text{-(Fe,Cr)}_{2,3}\text{N}$ ,  $\gamma'\text{-(Fe,Cr)}_4\text{N}$ , and  $\alpha''\text{-(Fe,Cr)}_8\text{N}$  phases.

**Table 2** Surface layer parameters for steels ion implanted at different ion beam current densities

Alloy	Ion current density, $\text{mA/cm}^2$	Depth of modified layer, $\mu\text{m}$	Surface microhardness, MPa	Bulk microhardness, MPa	Main phases
40X quenching	Virgin	–	6700	6700	$\alpha\text{-Fe}$
	1	40*	9900	3700	$\epsilon\text{-Fe}_{2-3}\text{N}$ ; $\gamma'\text{-Fe}_4\text{N}$ ; $\alpha\text{-Fe}$
	1,5	30*	9500	4000	Same
	2	20*	9500	4200	Same
40X13 quenching	Virgin	–	6000	6000	$\alpha\text{-Fe}$
	1	18 – 20	12000	5000	$\epsilon\text{-(Fe,Cr)}_{2-3}\text{N}$ ; $\gamma'\text{-Fe}_4\text{N}$ ; $\alpha''\text{-Fe}_8\text{N}$ ; $\alpha_{\text{N}}$
	1,5	18 – 20	13000	5000	Same
	2	15 – 20	12500	5200	Same

**Fig. 2** – Microstructure of the surface layer for nitrogen ion implanted 40X steel: (a) – quenched steel; (b) – annealed steel



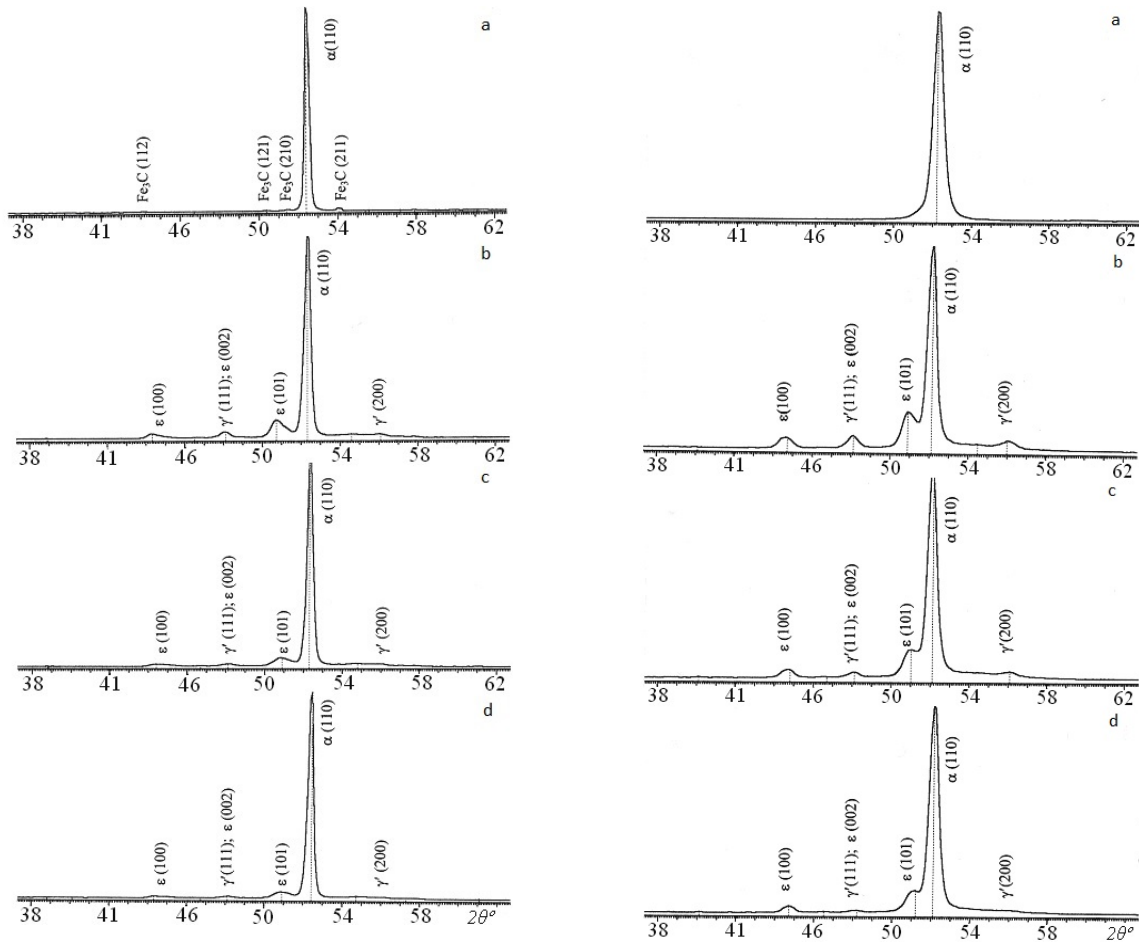


**Fig. 3.** Segments of X-ray diffraction spectra (CoK $\alpha$ ) from surface layers of 40X steel (left column – preliminary annealed steel; right column – preliminary quenched steel): a – virgin bocks; b – ion implantation at dose rate  $j=1 \text{ mA/cm}^2$ ; c –  $j=1,5 \text{ mA/cm}^2$ ; d –  $j=2 \text{ mA/cm}^2$

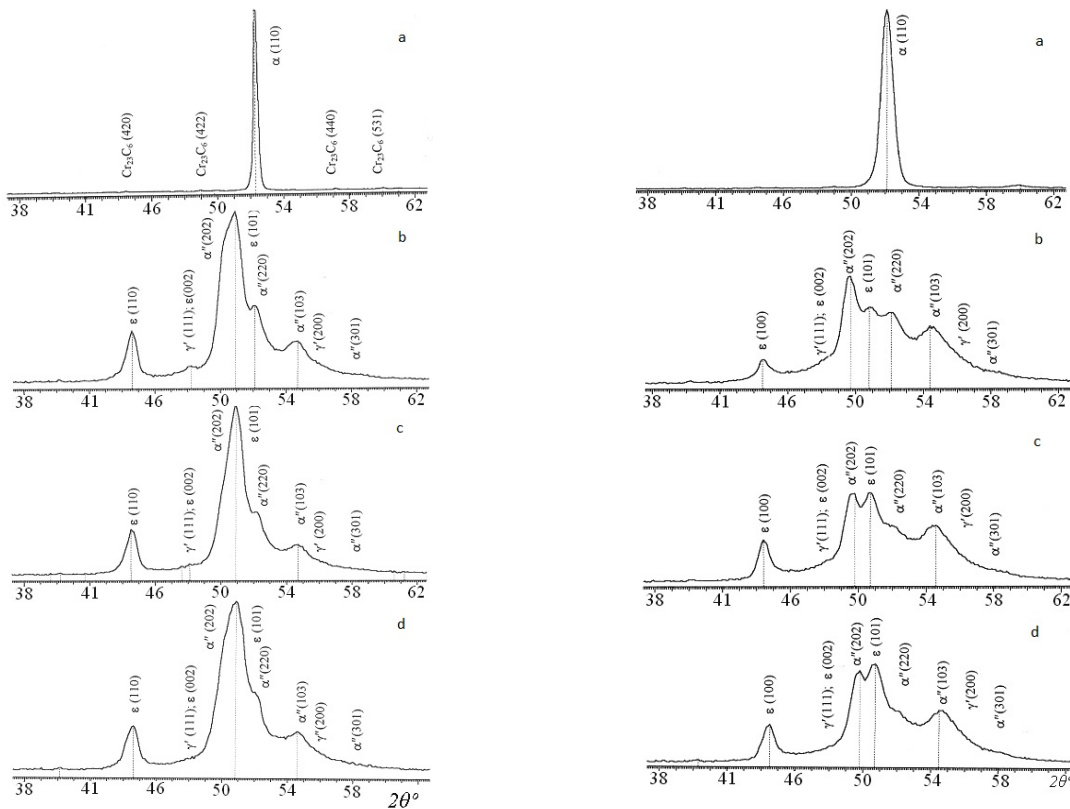


**Fig. 4.** Segments of X-ray diffraction spectra (CoK $\alpha$ ) from surface layers of 40X13 steel (left column – preliminary annealed steel; right column – preliminary quenched steel): a – virgin bocks; b – ion implantation at  $j=1 \text{ mA/cm}^2$ ; c –  $j=1,5 \text{ mA/cm}^2$ ; d –  $j=2 \text{ mA/cm}^2$

After annealing 40X13 steel had a bainite structure, containing  $\alpha$ -phase,  $\text{Cr}_{23}\text{C}_6$ ,  $\text{Cr}_7\text{C}_3$  carbides (traces). The lattice parameter of  $\alpha$ -phase was 0.2870 nm and surface microhardness of the steel  $H_{\mu} = 2400$  MPa. Ion implantation at a low dose rate ( $1 \text{ mA/cm}^2$ ) influenced 14-16 nm surface layer and increased its surface microhardness up to  $H_{\mu} = 12000$  MPa. Bulk microhardness of ion implanted block fell down to  $H_{\mu} = 5000$  MPa. X-ray diffraction of blocks revealed a near-surface layer containing  $\alpha''$ - $\text{Fe}_8\text{N}$ ;  $\epsilon$ - $(\text{Fe}, \text{Cr})_2\text{N}$ ;  $\gamma'$ - $\text{Fe}_4\text{N}$  and  $\alpha_{\text{N}}$  phases. The concentration of  $\alpha''$ -phase was lower and concentration of  $\epsilon$ -phase higher, than

in the case of quenched steel. Dose rate increase up to 1.5 and  $2 \text{ mA/cm}^2$  resulted in a doped layer with 8-10  $\mu\text{m}$  thickness (Fig. 4d). Surface microhardness increased up to  $H_{\mu} = 12500$ - $14000$  MPa. X-ray diffraction of annealed blocks ion implanted at high dose rates revealed a near-surface layer containing nitrogen rich  $\epsilon$ - $(\text{Fe}, \text{Cr})_2\text{N}$  phase. Concentrations of nitrogen poor  $\alpha''$ - and  $\gamma'$ -phases were dramatically lower than in the case of quenched steel.

Data for surface microhardness versus distance from the implanted surface of blocks are presented in Fig. 5

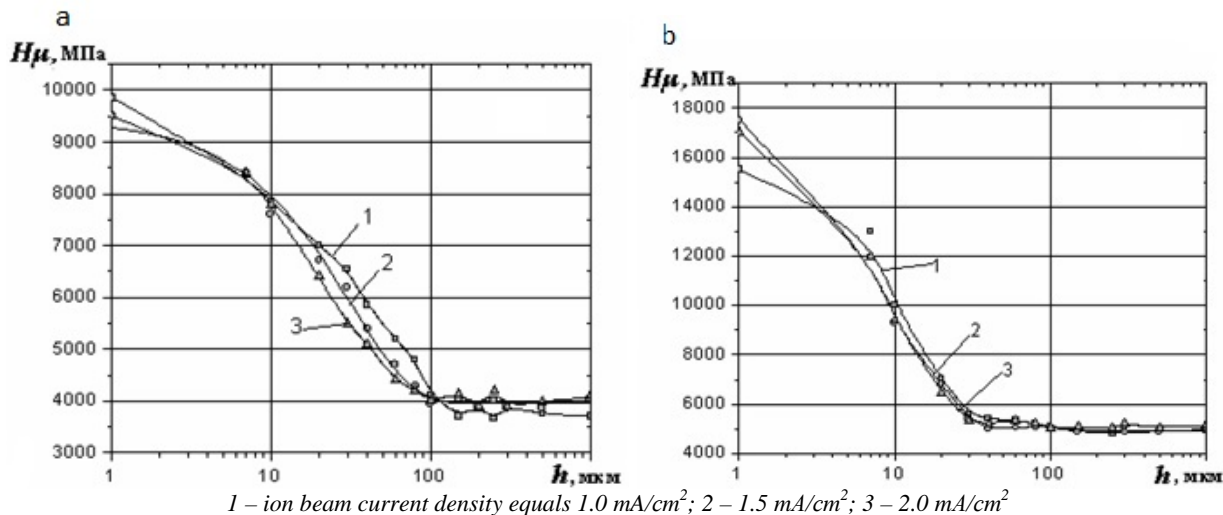


Fig 5 – Surface microhardness of quenched 40X (a) and 40X13 (b) steels implanted with nitrogen versus depth from the surface  
1 – ion beam current density equals  $1.0 \text{ mA/cm}^2$ ; 2 –  $1.5 \text{ mA/cm}^2$ ; 3 –  $2.0 \text{ mA/cm}^2$

The depth of modified layer in quenched 40X13 steel is determined mainly by the ion fluence and does not depend significantly on the processing time. Comparatively low defect concentration in annealed steel results in a comparatively low diffusivity of nitrogen. Radiation-induced defects do not compensate the lack of high defect concentration typical for martensite structure. As a consequence the depth of modified layer falls down, and nitrogen-rich  $\epsilon$ -phase inclusions dominate in the surface layer. The depth of modified layer increases with the time of treatment.

Data obtained show that dose rate is an important ion beam treatment parameter. As the role of diffusion during elevated-temperature, low-energy implantation exceeds that of simple, ballistic ion delivery, virgin microstructure and chemical composition of the surface layer were extremely important.

Chromium concentration dramatically influences parameters of the implanted layer. The thickness of modified layer on the surface of 40X13 steel was significantly smaller than on the surface of 40X steel. The microstructure of ion implanted layers was also significantly different with high-strength non-brittle tetragonal  $\alpha''$ - $(\text{Fe}, \text{Cr})_8\text{N}$  phase observed only for nitrogen implanted chromium-rich 40X13 steel.

Processing of 40X steel with low nitrogen solubility in martensite, results in a prompt formation of surface nitrated layer. This layer consists of nitrides and slows down further saturation of the bulk material because of slow nitrogen diffusivity. Diffusivities of nitrogen in  $\gamma'$ - and  $\epsilon$ -phases were correspondingly 25 and 6 times smaller than those for martensite). Nitrogen diffu-

sion in the bulk material takes place mainly along grain, twin, low-angle boundaries, and dislocations. The depth of doped layer for both quenched and annealed steels was controlled by nitrogen diffusivity and increased for a long processing time (low dose rates). Low dose rates also insured higher concentration of nitrides with dominating of the hard wear-resistant nitrogen poor  $\gamma'$ - $\text{Fe}_4\text{N}$  phase. On the contrary high dose rates' result in thin modified layers and low concentrations of nitrides, essentially of nitrogen poor  $\gamma'$ - $\text{Fe}_4\text{N}$  inclusions. Steel hardening led to a dramatic increase of defect concentration and intensified nitrogen diffusivity with consequent variation of nitride morphology.

In the case of chromium-rich 40X13 blocks the kinetics of ion-implanted layer formation looks dramatically different. High concentration of chromium results in a thinner doped layer with a different phase composition. High concentration of crystal defects favors solubility and diffusivity of nitrogen during ion implantation and results in the development of inner nitriding zone, containing nitrogen-doped martensite with inclusions of nitrides. Concentrations of nitrides and nitrogen-rich phases increase towards the surface. Precipitates of tetragonal  $\alpha''$ -phase ( $\text{Fe}_8\text{N}$ ), with the regular arrangement of nitrogen atoms in a phase lattice, were observed in the surface layer. Low dose rate favors formation of nitrogen poor  $\gamma'$ - $\text{Fe}_4\text{N}$  and  $\alpha''$ - $\text{Fe}_8\text{N}$  phases in quenched 40X13 steel. Schematic to illustrate dose rate influence on parameters and properties of modified surface layer is presented in Fig. 6.

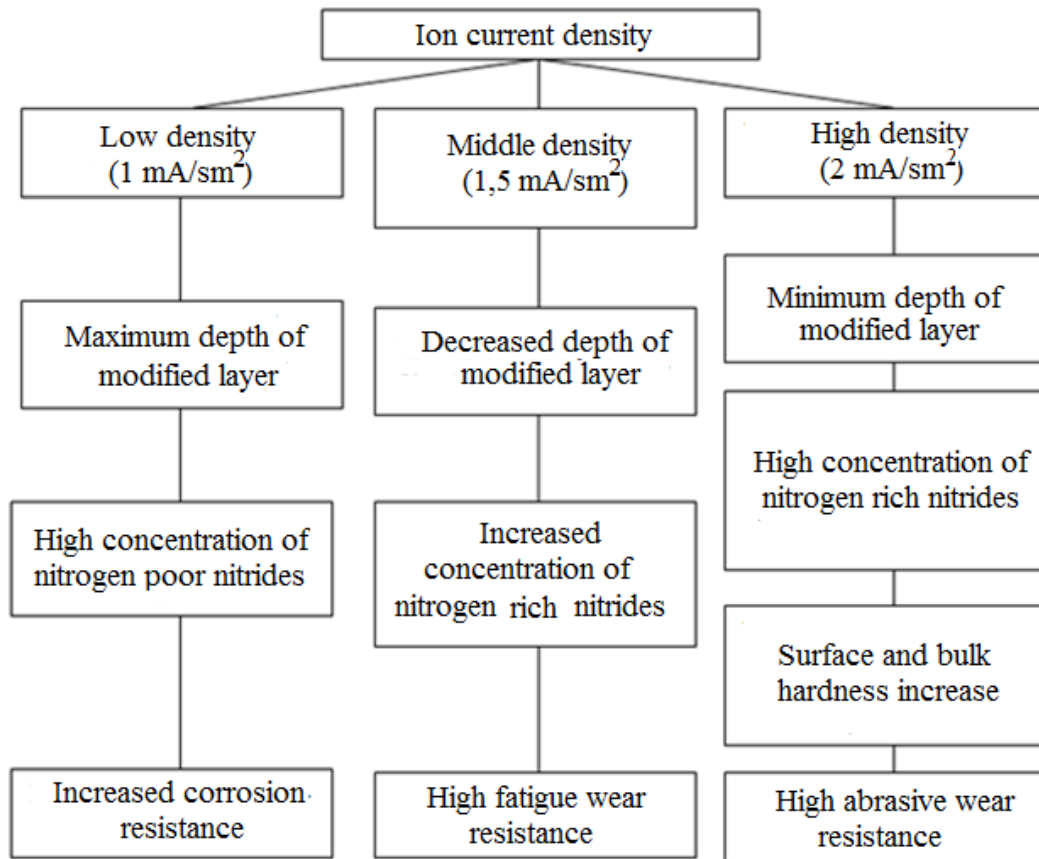


Fig. 4 – Schematic to illustrate influence of ion beam current density on parameters and properties of steel surface layers

### Conclusions

The data presented demonstrate that dose rate, chemical composition and initial surface microstructure are extremely important for low-energy, elevated-temperature ion implantation, when the role of diffusion exceeds that of ballistic penetration and the thickness of nitrated layer extends far beyond the ballistic implantation range.

Microstructure and kinetics of the surface modification dramatically differ for steels with low and high concentration of chromium atoms. The implanted layer on the surface of 40X steel consists of  $\epsilon$ - and  $\gamma'$ -phases and its thickness scales with the processing time. Nitrogen diffusion along grain, twin, low-angle boundaries, and dislocations takes place during ion-beam processing of both quenched and annealed 40X steel.

In the case of 40X13 blocks dose rate does not influence the thickness of implanted layer. Fast diffusivity of nitrogen in quenched chromium-rich steel 40X13 as well as radiation-stimulated diffusion explain formation of comparatively deep modified layers at dose rates 1.5 mA/cm<sup>2</sup> and 2.0 mA/cm<sup>2</sup>. Tetragonal phase with low concentration of nitrogen was detected in the surface layer of ion implanted 40X13 blocks.

Preceding block hardening increased the density of crystal defects, increased nitrogen diffusivity, and led to homogeneous nitrogen distribution in the surface layer. As a consequence high-strength nitrogen poor inclusions dominated in the doped layer of implanted steels. Low inherent crystal defect concentration after annealing results in low diffusivity of implanted species, thin modified layers, and formation of comparatively brittle nitrogen-rich  $\epsilon$ -phase.

### Acknowledgment

This work is supported by the Belarusian Republican Foundation for Fundamental Research under the Grant T 16P218.

### References

1. P. J. Wilbur and L.O. Daniels, *Vacuum*, **36**, No. 1-3, (1986) 5-9.
2. A.V. Byeli, S.K. Shykh, V.V. Khatko, *Wear*, **159**, (1992) 185-190.
3. A.V. Byeli, O.V. Lobodaeva, S.K. Shykh, V.A. Kukareko, *Wear*, **181-183**, (1995) 632-637.
4. W.S. Sampath and P.J. Wilbur, *Mat. Res. Soc. Symp. Proc.*, **93**, (1987) 349-359.
5. D.L. Williamson, R. Wei, P.J. Wilbur, *Nuclear Instrum. Meth. Phys. Res.*, **B56/57**, (1991) 625-629.